Talanta 288 (2025) 127711

Contents lists available at ScienceDirect

Talanta

journal homepage: www.elsevier.com/locate/talanta

Benzoquinone-modified vertically aligned mesoporous silica for ratiometric electrochemical detection of diclofenac

Wafa Aidli, Silvia Comis, Luigi Falciola, Valentina Pifferi *

Dipartimento di Chimica, Università degli Studi di Milano, via Golgi 19, 20133, Milano, Italy

ARTICLE INFO

Handling editor: Agata Michalska

Keywords:
Nanoporous materials
Electrochemical assisted self-assembly
Thiol click chemistry
Ratiometric sensing
Environmental monitoring
Diclofenac analysis

ABSTRACT

A ratiometric electrochemical sensor featuring a benzoquinone-modified vertically aligned mesoporous silica film (BQ/VMSF) has been developed for the accurate detection of diclofenac (DCF), a widely utilized non-steroidal anti-inflammatory drug. The design process employed the Electrochemical assisted self-assembly (EASA) technique to grow a thiol-functionalized mesoporous silica film on a carbon screen-printed electrode, which was further modified with benzoquinone via click chemistry. Characterization using Transmission Electron Microscopy (TEM), Fourier-Transform Infrared Spectroscopy (FTIR), Cyclic Voltammetry (CV), and Electrochemical Impedance Spectroscopy (EIS) confirmed the successful synthesis and optimal functionality of the mesoporous structure. In this configuration, benzoquinone serves as an internal redox reference, generating one redox signal, while the electrochemical oxidation of diclofenac produces a second redox signal. The sensor's output is derived from the ratio of these two signals, I_{DCF}/I_{BQ}, enhancing its sensitivity and selectivity for diclofenac detection. The sensor, tested through Differential Pulse Voltammetry (DPV), exhibited a linear response range from 1 to 10 μM for diclofenac and a remarkably low limit of detection (LOD) of 0.73 μM. Application of the sensor for diclofenac analysis in pharmaceutical formulations demonstrated recovery rates ranging from 97.68 % to 101.79 % and relative errors below 2.32 %, affirming its practical utility.

1. Introduction

Diclofenac (DCF), a commonly used non-steroidal anti-inflammatory drug (NSAID), is recognized for its effectiveness in managing rheumatic discomfort and joint inflammation in both human and veterinary medicine. Despite its therapeutic benefits, DCF's widespread use has led to notable environmental repercussions. Approximately 75 % of the drug consumed infiltrates aquatic ecosystems, a consequence of its hydrophilic nature and resistance to natural degradation processes [1]. The presence of DCF in various water bodies has ignited concerns due to its potential to disrupt aquatic ecosystems [2,3], and pose health risks to humans, including gastrointestinal, renal, and cardiovascular issues [4].

The environmental and health implications of DCF underscore the imperative for precise, yet accessible, analytical techniques for its detection. While traditional methods like chromatography[5–8], spectrophotometry [9] and capillary electrophoresis [10] offer precision, their complexity, cost, and time consumption limit their practicality for frequent monitoring. Electrochemical approaches, capitalizing on DCF's electroactive nature [11], present a viable alternative, combining high sensitivity and specificity with simplicity, affordability, and ease of use [12]. These attributes make electrochemical methods particularly suited for the routine surveillance of DCF, facilitating timely identification and mitigation of its environmental and health impacts.

Extensive research has been devoted to the electrochemical detection of diclofenac, utilizing electrodes enhanced with various nanomaterials to boost sensitivity[13–15]. However, a significant challenge persists: the fouling of electrode surfaces. This issue is particularly acute in NSAID detection, including diclofenac, where it can severely diminish sensor sensitivity and result reliability [16]. Conventional strategies to mitigate fouling, such as applying protective coatings, often fall short when the analyte itself, such as DCF, is responsible for fouling [17]. This challenge necessitates innovative solutions that preserve electrode functionality without sacrificing analytical precision.

Mesoporous silica nanomaterials, particularly Vertically-aligned Mesoporous Silica Films (VMSF), have been used to address electrode fouling issues. Pioneering work by Walcarius and his team has demonstrated the efficacy of mesoporous silica films in mitigating fouling problems, especially when dealing with large biomolecules [18]. In fact,

This article is part of a special issue entitled: Electroanalysis published in Talanta.

* Corresponding author.
E-mail address: valentina.pifferi@unimi.it (V. Pifferi).

https://doi.org/10.1016/j.talanta.2025.127711
Received 18 July 2024; Received in revised form 3 February 2025; Accepted 7 February 2025
Available online 12 February 2025

VMSF distinguishes itself with its vertically oriented, uniformly sized nanochannels, offering high pore density, tunable thickness, and robust mechanical and chemical stability. These characteristics enable VMSF to perform selective filtering based on size, charge, and lipophilicity, thereby providing exceptional anti-fouling and anti-interference properties. VMSF modified electrodes were used for electrochemical analyzing small molecules in complex samples [19,20]. This was exemplified in a study by Wang et al. [21] where a VMSF-modified glassy carbon electrode detected doxorubicin in unprocessed human whole blood, demonstrating the material's effective antifouling capabilities. Additionally, the high surface area and the vertically channels of VMSF support rapid mass transport while naturally preventing analyte buildup [22]. The versatility of VMSF is further augmented by its potential for functionalization, enabling the incorporation of various organic molecules or nanoparticles to tailor the material's properties for specific sensing applications.

Parallelly, the adoption of ratiometric electrochemical sensing has been found to boost sensor's accuracy [23,24]. Different from the conventional single signal sensors, ratiometric electrochemical sensors use the ratio of two current signal responses at distinct redox potentials as the final signal output. One signal derives from the electroactive analyte, while the other is attributed to an internal reference probe (e.g., thionine [25], methylene blue [26], ferrocene [27]). Since the reference probe and target analyte are affected by the same sensing environment, ratiometry offers an inner self-calibration that further improves accuracy and sensitivity [28].

Inspired by the concepts discussed, we developed an innovative ratiometric electrochemical sensor that incorporates a benzoquinone-modified vertically aligned mesoporous silica film (BQ-VMSF) for the detection of diclofenac. The design of this sensor involves the electrochemical deposition of a mercapto-modified VMSF onto a screen-printed electrode (SPCE), further modified with benzoquinone molecules. The chosen design uses Benzoquinone's redox behavior to provide a reliable reference signal. DCF was successfully oxidized on the modified electrode and a distinct redox signal was produced. The final sensor output is determined by the ratio of the diclofenac to benzoquinone signals, significantly boosting sensitivity and selectivity. The BQ-VMSF modified SPCE has demonstrated its efficacy in analyzing diclofenac in pharmaceutical samples.

2. Materials and methods

2.1. Materials and reagents

Tetraethoxysilane (98 %), (3-Mercaptopropyl)trimethoxysilane (95 %), Cetyltrimethylammonium bromide (≥98 %), Sodium nitrate (≥99.0 %), Hydrogen peroxide (30 % (w/w) in H_2O), Hydrochloric acid (37 %), Ethanol (99 %), Diclofenac sodium salt, Citric acid, Polyvinylpyrrolidone, Cellulose, Glucose, Urea, were purchased from Sigma-Aldrich and used without further purification.

2.2. Electrochemical pre-activation of SPCE

To ensure the Screen-Printed Carbon Electrodes (SPCEs) were primed for the subsequent silica film application, a critical pre-activation step was executed as per the recommendations in the literature [29]. The SPCEs were subjected to 25 repetitive cyclic voltammetry scans at a scan rate of 10 mV/s, within the voltage range of +1.0 to −0.7 V (vs. Ag), all conducted in a solution of 10 mM H_2O_2, in a 0.1 M phosphate buffer solution at pH 7. Following the activation, the electrodes were thoroughly rinsed with deionized water and left to dry in ambient air.

2.3. Growth of vertically-ordered mesoporous silica films (VMSF)

The synthesis of VMSFs on SPCEs was meticulously carried out using the Electrochemically assisted self-assembly (EASA) technique, following the established protocol by Walcarius and co-workers [30,31] (See Fig. 1). A precursor solution was first prepared. We combined a 0.1 M aqueous solution of $NaNO_3$ with ethanol in a 1:1 vol ratio. To this mixture, we added Tetraethoxysilane (TEOS) and cetyltrimethylammonium bromide (CTAB) to achieve final concentrations of 100 mM and 32 mM, respectively. The pH was adjusted to 3.0 by adding HCl, and the solution was hydrolyzed with continuous stirring at room temperature for 2.5 h.

For the growth of VMSFs, the SPCE was positioned horizontally, as a canvas for our nanostructure. We deposited 80 μL of the precursor solution onto the electrode surface. By applying a voltage of −2.2 V for 30 s the growth process initiated. Subsequently, the electrode was promptly removed, thoroughly rinsed with water, and dried under a stream of nitrogen. To ensure the robust cross-linking of the silica network, the electrode underwent an overnight aging process at 100 °C. The removal of surfactant micelles (CTAB) from the nanochannels was accomplished by immersing the CTAB/VMSF/SPCE in a 0.1 M HCl-ethanol solution under moderate stirring for 5 min. This yielded the final VMSF/SPCE.

In the case of benzoquinone functionalized films, the precursor solution contained MPTMS silane, and the concentration was systematically varied at 10 %, 15 %, 20 %, and 30 % by weight of MPTMS/TEOS, maintaining a total silane concentration of 100 mM. Following the removal of CTAB, the exposed thiol groups facilitated the attachment of benzoquinone molecules within the mesopores through a click chemistry reaction [32]. The functionalized electrode was immersed in a 5 mM benzoquinone solution for 1 h, ensuring the thorough incorporation of the benzoquinone. A final rinse with water and drying under nitrogen flow completed the synthesis, yielding the benzoquinone-modified VMSF/SPCE ready for electrochemical applications.

2.4. Measurements and instrumentations

ATR-FTIR spectra was recorded using a Nicolet 380 spectrophotometer (Thermo Electron Corporation, Waltham, MA, USA) between 4000 and 400 cm^{-1}. The spectrum was obtained as the result of 64 accumulations. Transmission Electron Microscope (TEM) analyses were performed on a JEOL JEM 3010UHR microscope operating at 300 kV. Samples were prepared by mechanically removing (scraping) some pieces of the mesoporous films, which were dispersed in absolute ethanol solution and deposited on 200 mesh Cu "holey" carbon grids and dried at room temperatures before the analysis.

Electrochemical analyses were performed on bare and modified disposable DropSens carbon screen printed electrode (101) and using a PGstat30 potentiostat/galvanostat (Autolab, The Netherlands) equipped with FRA module and controlled with NOVA 2.0 software. Cyclic voltammetry (CV) and Differential pulse voltammetry (DPV) were performed at a scan rate of 50 mV s^{-1} and 10 mV s^{-1} respectively in 0.1 M PBS solution as a supporting electrolyte. Electrochemical impedance spectroscopy (EIS) was performed at 0 V applied potential, in the frequency range 0.1 Hz–100 kHz with amplitude 0.01 V in the presence of $Ru(NH_3)_6^{3+}$ redox probe (0.5 mM) in 0.1 M KCl solution. Impedance data were processed with Z-View 3.1 software. All measurements were made in triplicate.

2.5. Preparation of real samples

Real sample analysis was conducted using commercially available Diclofenac tablets, each containing 25 mg of the drug. The tablet was finely ground and dissolved in 50 cm^3 of Milli-Q water, followed by filtration to remove insoluble residues. The clear filtrate was then diluted in PBS (0.1 M, pH 7) to a final volume of 100 cm^3. The obtained solution was used as the analyte for diclofenac determination.

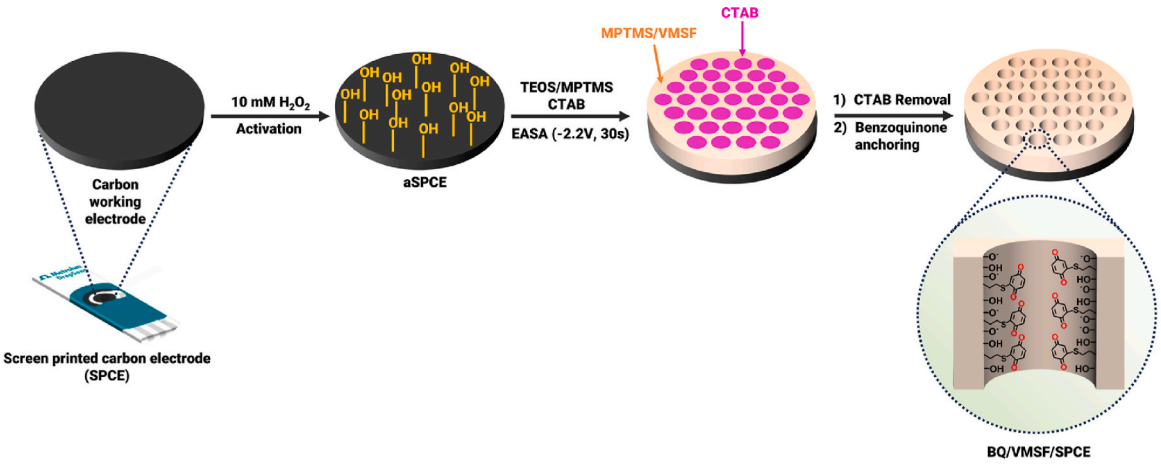

Fig. 1. Schematic Illustration of the preparation process for Benzoquinone-Modified Vertically Aligned Mesoporous Silica Film (BQ/VMSF) on Screen-Printed Electrodes.

3. Results and discussion

3.1. Structural and morphological characterization

Transmission electron microscopy (TEM) analysis provided definitive evidence of the highly ordered hexagonal pore structure characteristic of the synthesized vertically-ordered mesoporous silica films (VMSFs), as depicted in Fig. 2A. These top-view TEM images, obtained after delaminating the VMSF from the electrode surface, reveal a uniform pore size distribution with diameters ranging from 2 to 3 nm. The absence of defects across significant portions of the film underscores the precision of the electrochemical assisted self-assembly process employed in the VMSF fabrication [33].

Fourier Transform Infrared (FTIR) spectroscopy further elucidated the chemical composition and structural integrity of the VMSFs. Spectral analysis before and after the removal of the CTAB surfactant provided insights into the mesoporous silica framework (Fig. 2B). The observed strong absorption band at 1052 cm^{-1}, attributed to Si–*O*–Si stretching vibrations, alongside distinct bands at 952 cm^{-1} and 790 cm^{-1} corresponding to Si–*O*–H and Si–O stretching vibrations respectively, confirm the siliceous nature of the VMSF. The bending vibration of Si–O bonds was identified at 427 cm^{-1}, with a broad absorption band at 3365 cm^{-1} indicating the presence of Si–*O*–H groups [34].

The initial presence of CTAB within the VMSF was confirmed through the identification of $–CH_2$ symmetric and asymmetric stretching vibrations at 2919 and 2874 cm^{-1}, respectively, and a bending mode of $–CH_2$ at 1460 cm^{-1}. The disappearance of these peaks following CTAB extraction, coupled with the emergence of a new peak at 1632 cm^{-1} corresponding to –OH groups, likely signifies physically adsorbed water molecules [35]. Overall, the characteristic siliceous bonds remained intact, highlighting the structural resilience of the VMSF in aqueous and acidic environments.

3.2. Optimization of VMSFs

Critical parameters such as EASA time deposition and MPTMS ratio were varied to electrochemical characterization, using both CV and EIS in the presence of $Ru(NH_3)_6^{3+}$ serving as the redox probe. The strategic selection of a cationic probe was made, considering the negative charge of the prepared VMSFs [36].

Initially, a sequence of activated SPCEs underwent modification with VMSFs, employing deposition times that varied from 5 to 30 s. This set of experiments excluded MPTMS from the precursor solution. Electrochemical responses were assessed using CV and EIS, with 0.5 mM Ru

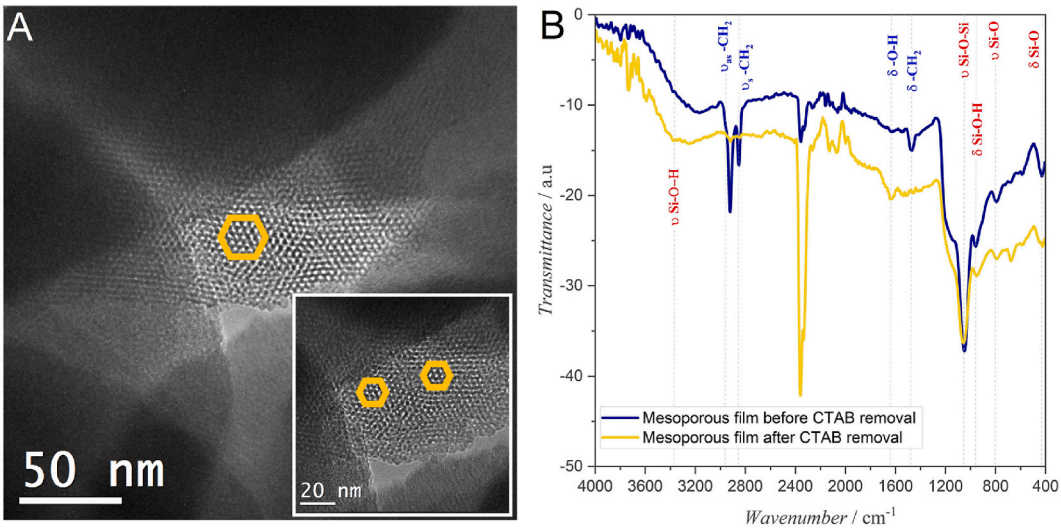

Fig. 2. Structural and morphological characterization of VMSF. (A)TEM images of the VMSF at various magnifications. (B) FTIR spectra of VMSF before and after CTAB removal.

$(NH_3)_6^{3+}$, both before and after the removal of the surfactant CTAB, as illustrated in Fig. 3.

Fig. 3A elucidates distinct redox peaks at + 0.025 V and - 0.125 V, corresponding to the oxidation and reduction of $Ru(NH_3)_6^{3+}$, respectively, on the activated SPCE. An observed decline in the redox activity of $Ru(NH_3)_6^{3+}$ was noted with an increase in EASA deposition time. For deposition times of 5 and 10 s, the electrodes retained moderate redox activity, implying partial surface coverage by the VMSF. In contrast, deposition durations of 15, 20, and 30 s led to a marked reduction in redox activity, suggesting more extensive surface coverage by the VMSF. Notably, the electrode with a 30 s deposition exhibited minimal to no redox activity, indicative of nearly complete surface coverage and the establishment of a uniformly distributed VMSF layer. These observations were further confirmed by EIS analysis. Fig. 3B presents Nyquist plot recorded before CTAB removal. As expected, the activated electrode exhibited a relatively low charge transfer resistance (R_{ct}) of 14 Ω cm^2. Upon modification with VMSF, a significant and gradual increase in charge transfer resistance was observed. The change in R_{ct} values is outlined as follows for varying deposition times: R_{ct} (5s) < R_{ct} (10s)< R_{ct} (15s) < R_{ct} (20s) < R_{ct} (30s) (see Table S1). The observed increase in R_{ct} with extended deposition times signifies a greater hindrance to charge transfer processes, indicative of the formation of denser and more expansive mesoporous layers on the working electrode surface.

Following the removal of CTAB, we conducted the same measurements on the VMSF-modified electrodes. The cyclic voltammograms depicted in Fig. 3C unequivocally showed a pronounced resurgence in the redox activity of $Ru(NH_3)_6^{3+}$, characterized by the distinct oxidation and reduction peaks typical of this redox probe. This clear recovery of redox signals confirms the electrodes' restored permeability to solution-phase redox probes post-CTAB extraction. Notably, we observed variations in the intensity of the peak currents, which we attribute to differing degrees of surface electrode coverage. Despite the electrode subjected to a 30-s deposition displaying lower peak intensity compared to the others, this reduction in intensity is sufficient to confirm the full restoration of electroactivity, all along with permeability of the electrode.

The Nyquist plots recorded after CTAB removal confirm the presence of a characteristic Warburg element, particularly at low frequencies (Fig. 3D). This presence indicates a diffusion process occurring at the electrode–electrolyte interface across all modified electrodes. The presence of a Warburg element across all the modified electrodes suggests that the mesoporous structure of the VMSF remains effective in facilitating diffusion post-CTAB removal. The data also demonstrate a progressive increase in the charge transfer resistance R_{ct} with longer deposition times of VMSF, ranging from 19 Ω cm^2 at 5 s to 39 Ω cm^2 at 30 s. Interestingly, a noticeable reduction in charge transfer resistance is observed across all VMSF-modified electrodes when comparing the

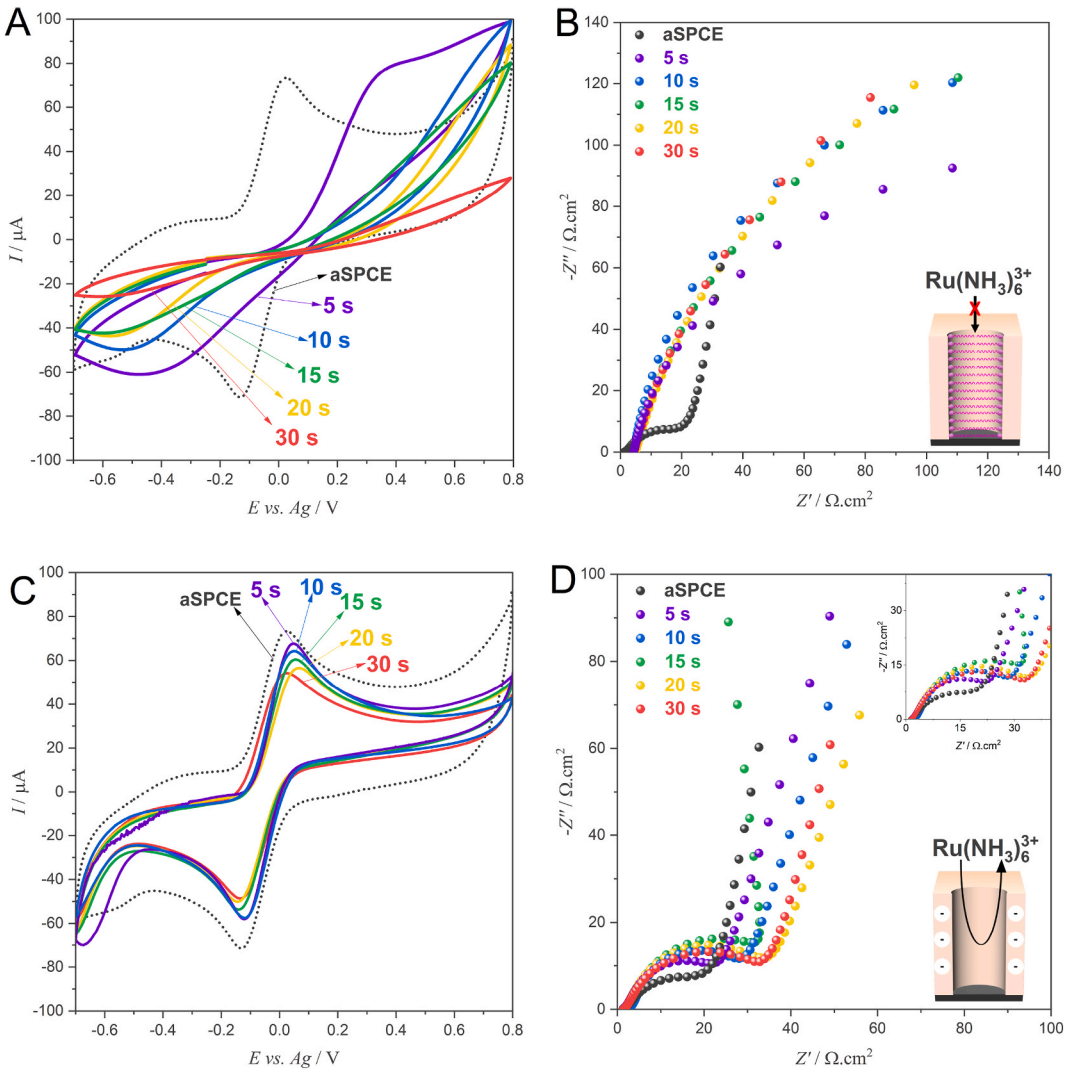

Fig. 3. Electrochemical properties of VMSF-modified electrodes at various deposition times (A) CV and (B) EIS analyses before CTAB removal, (C) CV and (D) EIS post-CTAB removal in the presence of 0.5 mM $Ru(NH_3)_6^{3+}$ in 0.1 M KCl solution.

states before and after CTAB removal. This decrease in R_{ct} is a positive indicator of the restored electroactivity of the electrodes. The slight increase in R_{ct} with 30 s deposition time can be attributed to the thicker mesoporous silica layers, which may introduce additional resistance to electron transfer, yet it does not impede the electroactivity of the electrode.

To optimize the functionalization of VMSFs, we assessed the effect of doping with 3-mercaptopropyltrimethoxysilane (MPTMS). We modified various electrodes with VMSFs incorporating different MPTMS ratios in the precursor solution, namely, 10 %, 15 %, 20 %, and 30 % relative to TEOS, alongside a control sample with 0 % MPTMS.

Cyclic voltammetry recorded after the removal of CTAB, as depicted in Fig. 4A, showed a decrease in peak current intensity with increasing MPTMS content when the electrodes were tested with the $Ru(NH_3)_6^{3+}$ redox probe. This inverse relationship suggests that the presence of MPTMS and the thiol groups within the mesoporous structure introduces steric hindrances that affect the electrode's electroactivity. The corresponding EIS data, presented in Fig. 4B, further supported these findings. The Nyquist plots revealed an increase in the diameter of the semicircles, indicative of heightened charge transfer resistance (R_{ct}), with the increment of MPTMS concentration. This trend is quantitatively substantiated by Table S3, which specifies that the R_{ct} for electrodes with 30 % MPTMS/TEOS doping is approximately 2.68 times greater than that of the undoped VMSF.

The efficacy of benzoquinone immobilization on electrodes was tested. After soaking the prepared MPTMS/VMSF-modified electrodes in a benzoquinone solution, we employed both cyclic voltammetry (CV) and differential pulse voltammetry (DPV) for assessment. The voltammograms, displayed in Fig. 4C, exhibit a clear redox couple corresponding to the oxidation of hydroquinone (HQ) to benzoquinone (BQ) at +0.05 V vs. Ag and the reduction of BQ to HQ at −0.09 V vs. Ag. This redox interconversion reflects the stable and reversible behavior of the immobilized BQ/HQ system.

In DPV measurements (Fig. 4D), a pronounced peak at −0.03 V vs. Ag was observed, which is attributed to the oxidation of hydroquinone (HQ) generated during the reduction of benzoquinone under negative potential conditions. The intensity of this oxidation signal increased with the MPTMS content in the mesoporous silica film, reaching its highest value with the 30 % MPTMS/VMSF electrodes. This trend indicates that higher MPTMS content facilitates greater immobilization of benzoquinone molecules, enhancing the availability of hydroquinone for oxidation during the anodic sweep.

No significant hindrance to the redox activity was observed, suggesting that the mesoporous silica framework provides an effective

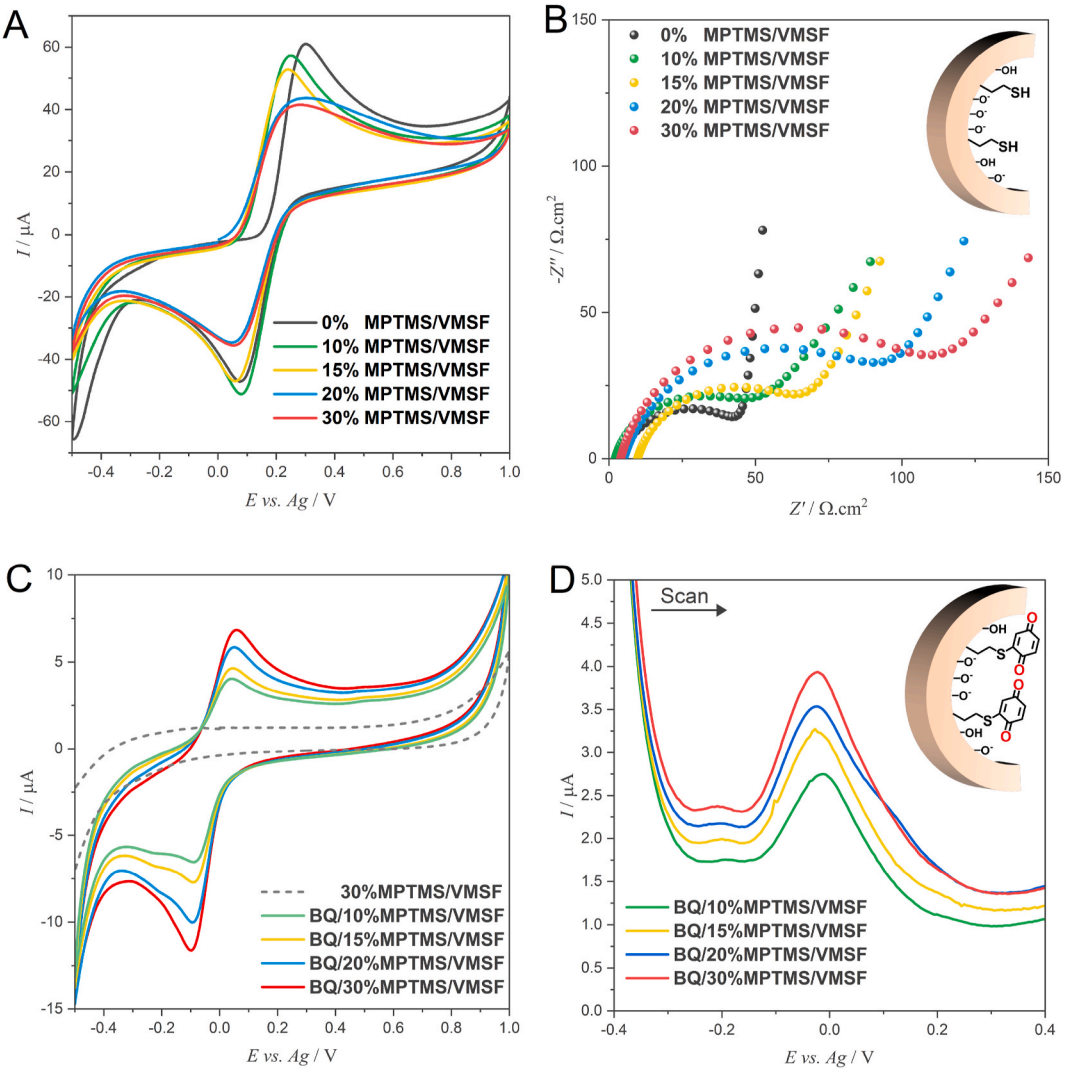

Fig. 4. Impact of MPTMS concentration on the electrochemical behavior of VMSF modified electrodes. (A) CV and (B) EIS of VMSF-modified electrodes with varying MPTMS percentages, conducted in 0.5 mM $Ru(NH_3)_6^{3+}$ in 0.1 M KCl solution. (C) CV and (D) DPV of different BQ/MPTMS/VMSFs modified electrodes conducted in 0.1 M PBS solution.

environment for the immobilized benzoquinone. Based on these findings, the BQ/30 % MPTMS/VMSFs grown for 30 s were adopted as the optimal film composition for electrode modification.

3.3. Analytical performance of the sensor

Differential pulse voltammetry (DPV) was performed in the presence of increasing concentrations of diclofenac, and the results are depicted in Fig. 5A.

The electrochemical oxidation of diclofenac DCF involves a one-electron transfer process that forms a reactive radical cation as the primary intermediate [37]. A discernible peak emerged at + 0.47 V vs. Ag, corresponding to the oxidation of diclofenac. Remarkably, this oxidation potential is significantly lower than typically reported values for diclofenac detection, indicating an electrocatalytic effect. For example, in a study using a silica modified glassy carbon electrode, diclofenac was detected at a higher potential of +0.75 V vs. Ag, which is approximately 85 mV lower than that observed on bare glassy carbon electrodes [38].

The DCF peak exhibited an increase current intensity with rising diclofenac concentration. In contrast, the signal for benzoquinone decreased as the diclofenac concentration increased, a phenomenon likely due to fouling effects within the mesoporous structure when diclofenac is added.

This behavior revealed a direct and proportional correlation between both peak signals and the concentration of Diclofenac, as illustrated in Fig. 5B. We established linearity between 1 and 10 μM, resulting in a calibration equation for diclofenac as follows:

$I_{DCF} = (3.168 \times 10^{-7}) \cdot C_{DCF} + (1.770 \times 10^{-6})$ $(R^2 = 0.988)$. The calculated limit of detection (LOD) for diclofenac, determined as $LOD = (3.29 \bullet s_y)/S$, where s_y is the residual standard deviation and S is the slope of the calibration plot, was found to be 1.11 μM.

In parallel, a calibration plot was also established according to the benzoquinone signal using the following equation:

$I_{BQ} = (-1.01 \times 10^{-7}) \cdot C_{DCF} + (3.379 \times 10^{-6})$ $(R^2 = 0.995)$. Using this calibration equation, we determined the limit of detection for diclofenac, derived from the linear regression analysis. The calculated LOD for diclofenac was found to be 0.68 μM. The lower LOD can be attributed to the fact that benzoquinone molecules are more confined to the electrode surface, which enhances signal stability. This stability, coupled with its higher electroactivity compared to diclofenac molecules, significantly increases the sensitivity of the signal, lowering the LOD.

Remarkably, the ratio of Diclofenac to Benzoquinone signals demonstrated a direct proportionality to the concentration of diclofenac, as evidenced by the linear regression established and depicted in Fig. 5C:

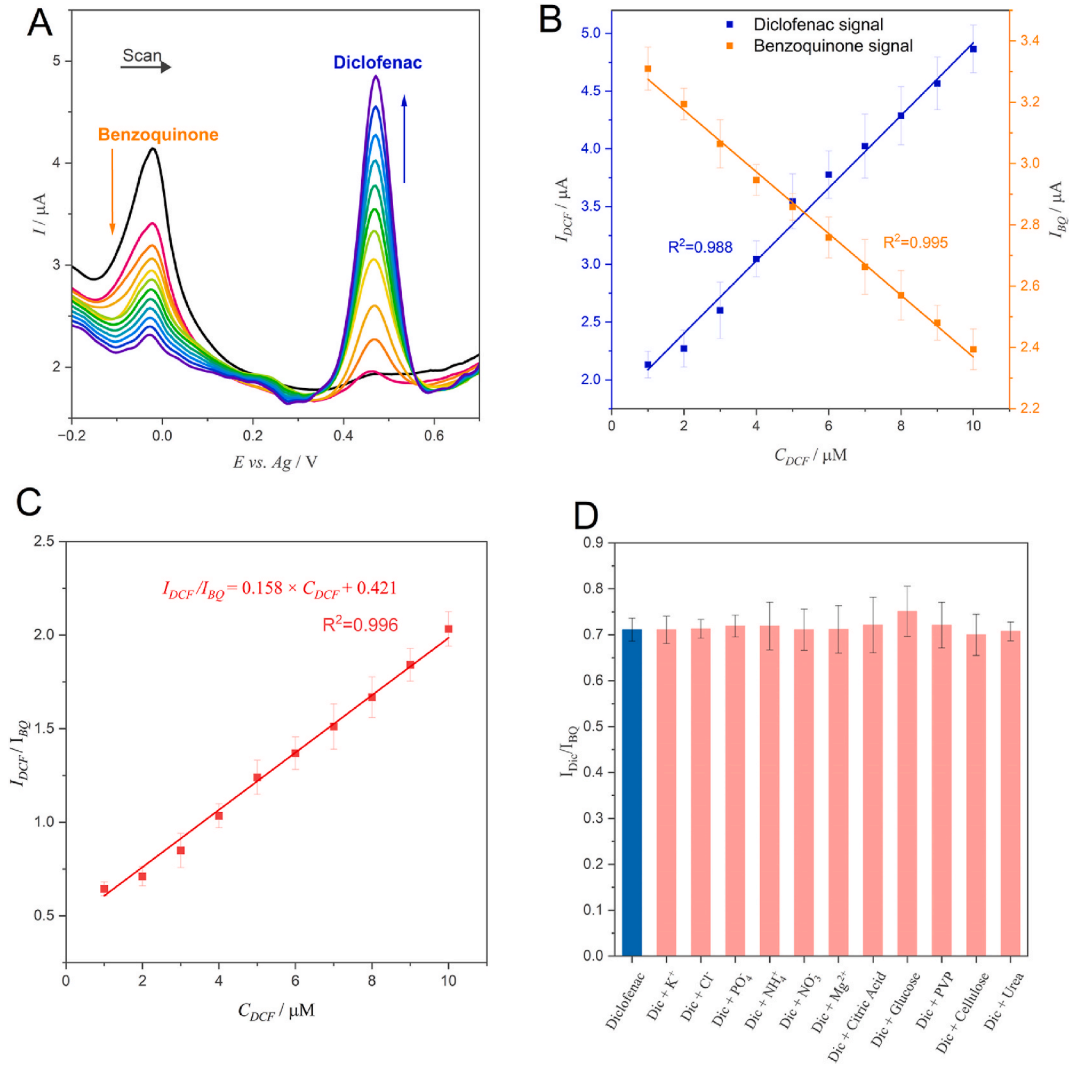

Fig. 5. (A) DPV measurements recorded in 0.1 M PBS at pH 7 with consecutive additions of Diclofenac form. (B) Calibration plots of both Benzoquinone and Diclofenac single signals. (C) Calibration plots of the ratio of Diclofenac and Benzoquinone signals. (D) electrochemical response of different electrodes in the presence of diclofenac (C_{DCF} = 2 μM) and common interferences ($C_{interferent}$ = 10 μM).

$I_{DCF/BQ} = 0.158 \cdot C_{DCF} + 0.421$ $(R^2 = 0.996)$. This linear relationship, with a high coefficient of determination (R^2), indicates a robust correlation between the ratio of Diclofenac to Benzoquinone signals and diclofenac concentration. Notably, the LOD for diclofenac within this ratiometric framework was even lower, at 0.73 μM.

The LOD achieved using the ratiometric sensing strategy (0.73 μM) demonstrates a significant improvement over the LOD obtained from direct detection of diclofenac (1.11 μM). This improvement highlights the enhanced sensitivity provided by the ratiometric approach, which effectively reduces variability by normalizing the diclofenac signal against the benzoquinone reference.

To assess the selectivity of the developed sensor in the presence of excipients, a series of DPV experiments were conducted in the presence of different interferent molecules commonly found in excipient formulas, including citric acid, glucose, urea, polyvinylpyrrolidone, cellulose, and others, as detailed in Fig. 5D. The DPV method revealed that the majority of these interferences did not significantly impact the ratiometric current response of the sensor. This robustness against various excipients suggests a high level of selectivity in the electrochemical detection of Diclofenac. Furthermore, we attribute the notable selectivity of the developed sensor to the inherent characteristics of the mesoporous silica film. The mesoporous structure not only imparts size selectivity but also contributes to charge selectivity. This dual mechanism enhances the sensor's ability to discriminate against interfering substances, reinforcing its specificity for the electrochemical detection of Diclofenac. The results affirm that the proposed sensor is specifically designed for the accurate detection of Diclofenac in its pharmaceutical formulations, demonstrating its efficacy in the presence of common excipients encountered in practical formulations.

The electroanalytical performance of the method described herein was further compared to other reported approaches for DCF quantification employing various modified electrodes, as summarized in Table 1. In terms of detectability, characterized by the limit of detection (LOD), our proposed method exhibits comparable or superior performance to many of the methods previously reported. A lower detection potential has been reached in comparison to the oether modified electrodes. A key strength of this work is the low detection potential of +0.47 V, which is the lowest among the compared methods, reducing interference and improving selectivity.

Table 1
Performance comparison of various DCF Electrochemical sensors utilizing modified electrodes.

Method	Sensing matrix	E_{DCF} (V)	Linear Range (μM)	LOD (μM)	Ref.
SWV	GCE/APTES-Amino-AT-Silica	+0.75	0.3–20	0.053	[38]
DPV	MWCNTs/PGE	+0.79	0.047–12.95	0.017	[39]
FIA-AD	3Ds-CM	+0.8	10–40	0.47	[40]
DPV	MIP-PANI/rGO/CPE	NA	15.7–251.5	3.46	[41]
DPV	MWCNT/TiO_2NP/CPE	+0.6	1.1–5000	0.33	[42]
LSV	f-MWCNT/PBWE	+0.5	0.1–100	0.07	[43]
DPV	Au–PtNPs/f-MWCNTs/GE	+0.6	0.5–1000	0.3	[44]
DPV	Tyrosine-CPE	+0.67	10–140	3.28	[45]
DPV	BQ/VMSF/aSPCE	+0.47	1–10	0.73	This work

GCE/APTES-Amino-AT-Silica: A glassy carbon electrode modified with an amino-attapulgite–mesoporous silica composite film. **MWCNTs/PGE:** A pencil graphite electrode modified by multiwalled carbon nanotubes. **3Ds-CM:** 3D printed support of acrylonitrile butadiene styrene insulating filament with a composite material (CM) based on graphite and nail polish. **MIP-PANI/rGO/CPE:** A carbon paste electrode modified with a Molecular imprinted polyaniline and reduced graphene oxide. **MWCNT/TiO_2NP/CPE:** A carbon paste electrode modified with Multiwalled carbon nanotubes and titanium dioxide nanoparticles. **f-MWCNT/PBWE:** carboxylated-multiwalled carbon nanotubes-ink paper based working electrode. **Au–PtNPs/f-MWCNTs/GE:** A gold elctrode modified by Functionalized multi-walled carbon nanotubes and gold-platinum bimetallic nanoparticles. **Tyrosine-CPE:** Tyrosine-modified carbon paste electrode. **SWV:** square wave voltammetry. **FIS-AD:** flow injection analysis system **LSV:** Linear sweep voltammetry. **DPV:** Differential pulse voltammetry.

Table 2
Results of the recovery test of diclofenac in pharmaceutical tablets.

Sample	Spiked (μM)	Found (μM)	Apparent Recovery (%)	Relative error %
Voltadvance® (25 mg)	0.00	1.67	99.53	0.47
	1.00	2.71	101.79	1.79
	2.00	3.68	100.09	0.09
	3.00	4.64	97.68	2.32

3.4. Determination of diclofenac in real sample

To assess the developed sensor's practicality, we tested its efficacy with *Voltadvance (*25 mg*),* the commercial tablet form of diclofenac in Italy. The sensor's performance, particularly in accurately quantifying diclofenac concentrations, was rigorously evaluated, and the results are presented in Table 2. The findings indicate that the sensor achieved satisfactory recovery rates and minimal relative errors, highlighting its reliability for diclofenac measurement in pharmaceutical products. The sensor exhibited apparent recovery rates between 97.68 % and 101.79 % for various spiked concentrations, while maintaining relative errors below 2.32 %. These outcomes not only attest to the sensor's trueness and precision but also to its robustness and adaptability for diclofenac's trace analysis in complex samples.

4. Conclusion

The development of a benzoquinone-modified vertically mesoporous silica film for ratiometric electrochemical detection presents a significant advancement in the analytical quantification of Diclofenac. This novel sensor system demonstrates a superior limit of detection, enhanced sensitivity, and remarkable selectivity compared to traditional single signal methods, owing to the synergistic integration of mesoporous silica's structural advantages and the ratiometric detection strategy. The meticulous optimization of electrode modification parameters and the comprehensive characterization of the sensor's electrochemical properties underscore its potential for application in complex environments. The successful application of this sensor in real pharmaceutical samples further validates its practical utility and reliability. This study not only contributes a valuable tool for Diclofenac monitoring but also highlights the broader applicability of mesoporous silica films in electrochemical sensor development.

CRediT authorship contribution statement

Wafa Aidli: Investigation, Formal analysis, Data curation, Writing, Conceptualization. **Silvia Comis:** Investigation. **Luigi Falciola:** Writing, Supervision, Resources, Methodology. **Valentina Pifferi:** Writing, Visualization, Supervision, Resources, Conceptualization.

Declaration of competing interest

The authors declare that they have no known competing financial interests or personal relationships that could have appeared to influence the work reported in this paper.

Acknowledgements

The authors acknowledge the Italian Ministry of Foreign Affairs and

International Cooperation (MAECI) for the grant awarded to W. Aidli. We also extend our sincere gratitude to Professor Alain Walcarius for hosting S. Comis within his research group at the University of Lorraine and for providing invaluable guidance on the synthesis of mesoporous silica.

Appendix A. Supplementary data

Supplementary data to this article can be found online at https://doi.org/10.1016/j.talanta.2025.127711.

Data availability

No data was used for the research described in the article.

References

[1] S. Schmidt, H. Hoffmann, L.A. Garbe, R.J. Schneider, Liquid chromatography–tandem mass spectrometry detection of diclofenac and related compounds in water samples, J. Chromatogr. A 1538 (2018) 112–116, https://doi.org/10.1016/J.CHROMA.2018.01.037.

[2] L. Lonappan, S.K. Brar, R.K. Das, M. Verma, R.Y. Surampalli, Diclofenac and its transformation products: environmental occurrence and toxicity - a review, Environ. Int. 96 (2016) 127–138, https://doi.org/10.1016/J.ENVINT.2016.09.014.

[3] P. Sathishkumar, R.A.A. Meena, T. Palanisami, V. Ashokkumar, T. Palvannan, F. L. Gu, Occurrence, interactive effects and ecological risk of diclofenac in environmental compartments and biota - a review, Sci. Total Environ. 698 (2020) 134057, https://doi.org/10.1016/J.SCITOTENV.2019.134057.

[4] N. Vieno, M. Sillanpää, Fate of diclofenac in municipal wastewater treatment plant - a review, Environ. Int. 69 (2014) 28–39, https://doi.org/10.1016/j.envint.2014.03.021.

[5] P. Paíga, A. Lolić, F. Hellebuyck, L.H.M.L.M. Santos, M. Correia, C. Delerue-Matos, Development of a SPE–UHPLC–MS/MS methodology for the determination of non-steroidal anti-inflammatory and analgesic pharmaceuticals in seawater, J. Pharm. Biomed. Anal. 106 (2015) 61–70, https://doi.org/10.1016/J.JPBA.2014.06.017.

[6] L. Lonappan, R. Pulicharla, T. Rouissi, S.K. Brar, M. Verma, R.Y. Surampalli, J. R. Valero, Diclofenac in municipal wastewater treatment plant: quantification using laser diode thermal desorption—atmospheric pressure chemical ionization—tandem mass spectrometry approach in comparison with an established liquid chromatography-electrospray ionization–tandem mass spectrometry method, J. Chromatogr. A 1433 (2016) 106–113, https://doi.org/10.1016/J.CHROMA.2016.01.030.

[7] P. Szpot, O. Wachełko, M. Zawadzki, Application of ultra-sensitive GC-QqQ-MS/MS (MRM) method for the determination of diclofenac in whole blood samples without derivatization, J. Chromatogr. B 1179 (2021) 122860, https://doi.org/10.1016/J.JCHROMB.2021.122860.

[8] E.D. Kovacs, L. Silaghi-Dumitrescu, M.H. Kovacs, C. Roman, Determination of the uptake of ibuprofen, ketoprofen, and diclofenac by tomatoes, radishes, and lettuce by gas chromatography–mass spectrometry (GC–MS), Anal. Lett. 54 (2021) 314–330, https://doi.org/10.1080/00032719.2020.1779278.

[9] P.C. Damiani, M. Bearzotti, M.A. Cabezón, A.C. Olivieri, Spectrofluorometric determination of diclofenac in tablets and ointments, J. Pharm. Biomed. Anal. 20 (1999) 587–590, https://doi.org/10.1016/S0731-7085(99)00052-7.

[10] C. Román-Hidalgo, M. Dvořák, P. Kubáň, & María, J. Martín-Valero, M. Ángel Bello-López, Direct capillary electrophoresis analysis of basic and acidic drugs from microliter volume of human body fluids after liquid-phase microextraction through nano-fibrous membrane, (n.d.). https://doi.org/10.1007/s00216-019-02225-y.

[11] R.N. Goyal, S. Chatterjee, B. Agrawal, Electrochemical investigations of diclofenac at edge plane pyrolytic graphite electrode and its determination in human urine, Sensor. Actuator. B Chem. 145 (2010) 743–748, https://doi.org/10.1016/j.snb.2010.01.038.

[12] W. Boumya, N. Taoufik, M. Achak, H. Bessbousse, A. Elhalil, N. Barka, Electrochemical sensors and biosensors for the determination of diclofenac in pharmaceutical, biological and water samples, Talanta Open 3 (2021) 100026, https://doi.org/10.1016/j.talo.2020.100026.

[13] M.M. Eteya, G.H. Rounaghi, B. Deiminiat, Fabrication of a new electrochemical sensor based on Au–Pt bimetallic nanoparticles decorated multi-walled carbon nanotubes for determination of diclofenac, Microchem. J. 144 (2019) 254–260, https://doi.org/10.1016/j.microc.2018.09.009.

[14] C. Slim, N. Tlili, C. Richard, S. Griveau, F. Bedioui, Amperometric detection of diclofenac at a nano-structured multi-wall carbon nanotubes sensing films, Inorg. Chem. Commun. 107 (2019) 107454, https://doi.org/10.1016/j.inoche.2019.107454.

[15] M. Shalauddin, S. Akhter, W.J. Basirun, S. Bagheri, N.S. Anuar, M.R. Johan, Hybrid nanocellulose/f-MWCNTs nanocomposite for the electrochemical sensing of diclofenac sodium in pharmaceutical drugs and biological fluids, Electrochim. Acta 304 (2019) 323–333, https://doi.org/10.1016/j.electacta.2019.03.003.

[16] S. Motoc, F. Manea, A. Iacob, A. Martinez-Joaristi, J. Gascon, A. Pop, J. Schoonman, Electrochemical selective and simultaneous detection of diclofenac and ibuprofen in aqueous solution using hkust-1 metal-organic framework-carbon nanofiber composite electrode, Sensors (Switzerland) 16 (2016), https://doi.org/10.3390/s16101719.

[17] P.K. Kalambate, J. Noiphung, N. Rodthongkum, N. Larpant, P. Thirabowonkitphithan, T. Rojanarata, M. Hasan, Y. Huang, W. Laiwattanapaisal, Nanomaterials-based electrochemical sensors and biosensors for the detection of non-steroidal anti-inflammatory drugs, TrAC, Trends Anal. Chem. 143 (2021) 116403, https://doi.org/10.1016/j.trac.2021.116403.

[18] M.B. Serrano, C. Despas, G. Herzog, A. Walcarius, Mesoporous silica thin films for molecular sieving and electrode surface protection against biofouling, Electrochem. Commun. 52 (2015) 34–36, https://doi.org/10.1016/J.ELECOM.2015.01.010.

[19] B. Cheng, L. Zhou, L. Lu, J. Liu, X. Dong, F. Xi, P. Chen, Simultaneous label-free and pretreatment-free detection of heavy metal ions in complex samples using electrodes decorated with vertically ordered silica nanochannels, Sensor. Actuator. B 259 (2018) 364–371, https://doi.org/10.1016/j.snb.2017.12.083.

[20] F. Yan, B. Su, Tailoring molecular permeability of nanochannel-micelle membranes for electrochemical analysis of antioxidants in fruit juices without sample treatment, Anal. Chem. 88 (2016) 11001–11006, https://doi.org/10.1021/acs.analchem.6b02823.

[21] M. Wang, J. Lin, J. Gong, M. Ma, H. Tang, J. Liu, F. Yan, Rapid and sensitive determination of doxorubicin in human whole blood by vertically-ordered mesoporous silica film modified electrochemically pretreated glassy carbon electrodes, RSC Adv. 11 (2021) 9021–9028, https://doi.org/10.1039/d0ra10000e.

[22] T. Nasir, G. Herzog, M. Hébrant, C. Despas, L. Liu, A. Walcarius, Mesoporous silica thin films for improved electrochemical detection of paraquat, ACS Sens. 3 (2018) 484–493, https://doi.org/10.1021/acssensors.7b00920.

[23] W. Aidli, D. Fumagalli, V. Pifferi, L. Falciola, From dual-mode to multi-modal electrochemical based sensors: a path toward accurate sensing, Curr. Opin. Electrochem. (2025) 101655, https://doi.org/10.1016/J.COELEC.2025.101655.

[24] T. Yang, R. Yu, Y. Yan, H. Zeng, S. Luo, N. Liu, A. Morrin, X. Luo, W. Li, A review of ratiometric electrochemical sensors: from design schemes to future prospects, Sensor. Actuator. B Chem. 274 (2018) 501–516, https://doi.org/10.1016/j.snb.2018.07.138.

[25] Q. Hao, L. Lu, X. Kan, Probe and analogue: double roles of thionine for aloe-emodin selective and sensitive ratiometric detection, Sensor. Actuator. B Chem. 292 (2019) 247–253, https://doi.org/10.1016/j.snb.2019.04.129.

[26] Y. Jiang, X. Xiao, C. Li, Y. Luo, S. Chen, G. Shi, K. Han, H. Gu, Facile ratiometric electrochemical sensor for in vivo/online repetitive measurements of cerebral ascorbic acid in brain microdiaysate, Anal. Chem. 92 (2020) 3981–3989, https://doi.org/10.1021/acs.analchem.9b05484.

[27] Y. Hu, X. Wang, C. Wang, P. Hou, H. Dong, B. Luo, A. Li, A multifunctional ratiometric electrochemical sensor for combined determination of indole-3-acetic acid and salicylic acid, RSC Adv. 10 (2020) 3115–3121, https://doi.org/10.1039/c9ra09951d.

[28] T. Yang, R. Yu, Y. Yan, H. Zeng, S. Luo, N. Liu, A. Morrin, X. Luo, W. Li, A review of ratiometric electrochemical sensors: from design schemes to future prospects, Sensor. Actuator. B Chem. 274 (2018) 501–516, https://doi.org/10.1016/j.snb.2018.07.138.

[29] M.I. González-Sánchez, B. Gómez-Monedero, J. Agrisuelas, J. Iniesta, E. Valero, Highly activated screen-printed carbon electrodes by electrochemical treatment with hydrogen peroxide, Electrochem. Commun. 91 (2018) 36–40, https://doi.org/10.1016/j.elecom.2018.05.002.

[30] N. Vilà, J. Ghanbaja, A. Walcarius, N. Vilà, A. Walcarius, J. Ghanbaja Institut, J. Lamour, Clickable bifunctional and vertically aligned mesoporous silica films, Adv. Mater. Interfac. 3 (2016) 1500440, https://doi.org/10.1002/admi.201500440.

[31] F. Yan, J. Chen, Q. Jin, H. Zhou, A. Sailjoi, J. Liu, W. Tang, Fast one-step fabrication of a vertically-ordered mesoporous silica-nanochannel film on graphene for direct and sensitive detection of doxorubicin in human whole blood, J Mater Chem C Mater 8 (2020) 7113–7119, https://doi.org/10.1039/d0tc00744g.

[32] W. Aidli, V. Pifferi, A. Mars, D. Marinotto, M. Longhi, A. Manfredi, A.H. Hamzaoui, L. Falciola, β-cyclodextrin based platform for bimodal detection of o-toluidine and cholesterol: electrochemical and fluorescence sensing, Electrochim. Acta 464 (2023) 142936, https://doi.org/10.1016/j.electacta.2023.142936.

[33] A. Walcarius, E. Sibottier, M. Etienne, J. Ghanbaja, Electrochemically assisted self-assembly of mesoporous silica thin films, Nat. Mater. 6 (2007) 602–608, https://doi.org/10.1038/nmat1951.

[34] M. Farajzadeh, H. Alamgholiloo, F. Nasibipour, R. Banaei, S. Rostamnia, Anchoring Pd-nanoparticles on dithiocarbamate- functionalized SBA-15 for hydrogen generation from formic acid, Sci. Rep. 10 (2020) 18188, https://doi.org/10.1038/s41598-020-75369-y.

[35] F. Krohm, H. Didzoleit, M. Schulze, C. Dietz, R.W. Stark, C. Hess, B. Stühn, A. Brunsen, Controlling polymerization initiator concentration in mesoporous silica thin films, Langmuir 30 (2014) 369–379, https://doi.org/10.1021/la404004f.

[36] F. Yan, X. Lin, B. Su, Vertically ordered silica mesochannel films: electrochemistry and analytical applications, Analyst 141 (2016) 3482–3495, https://doi.org/10.1039/c6an00146g.

[37] M.M. Cid-Cerón, D.S. Guzmán-Hernández, M.T. Ramírez-Silva, A. Galano, M. Romero-Romo, M. Palomar-Pardavé, New INSIGTHS on the kinetics and mechanism of the electrochemical oxidation of diclofenac in neutral aqueous medium, Electrochim. Acta 199 (2016) 92–98, https://doi.org/10.1016/J.ELECTACTA.2016.03.094.

[38] S.L.Z. Jiokeng, I.K. Tonle, A. Walcarius, Amino-attapulgite/mesoporous silica composite films generated by electro-assisted self-assembly for the voltammetric

determination of diclofenac, Sensor. Actuator. B Chem. 287 (2019) 296–305, https://doi.org/10.1016/j.snb.2019.02.038.
[39] G.P. Fard, E. Alipour, R.E. Ali Sabzi, Modification of a disposable pencil graphite electrode with multiwalled carbon nanotubes: application to electrochemical determination of diclofenac sodium in some pharmaceutical and biological samples, Anal. Methods 8 (2016) 3966–3974, https://doi.org/10.1039/c6ay00441e.
[40] T.P. Lisboa, W.B.V. de Oliveira, C.C. de Souza, R.S. Oliveira, M.A.C. Matos, R. C. Matos, Development of a 3D disposable device for the electrochemical determination of diclofenac in different matrices, Anal. Bioanal. Chem. 415 (2023) 357–366, https://doi.org/10.1007/s00216-022-04414-8.
[41] M. Mostafavi, M.R. Yaftian, F. Piri, H. Shayani-Jam, A new diclofenac molecularly imprinted electrochemical sensor based upon a polyaniline/reduced graphene oxide nano-composite, Biosens. Bioelectron. 122 (2018) 160–167, https://doi.org/10.1016/j.bios.2018.09.047.
[42] M. Franco-Guzmán, L.H. Mendoza-Huizar, G. Roa-Morales, C.A. Galán-Vidal, G. A. Álvarez-Romero, Voltammetric quantification of diclofenac using a modified CPE enriched with TiO2 nanoparticles and MWCNT, J. Electrochem. Soc. 168 (2021) 037502, https://doi.org/10.1149/1945-7111/ABE8B7.
[43] E. Costa-Rama, H.P.A. Nouws, C. Delerue-Matos, M.C. Blanco-López, M. T. Fernández-Abedul, Preconcentration and sensitive determination of the anti-inflammatory drug diclofenac on a paper-based electroanalytical platform, Anal. Chim. Acta 1074 (2019) 89–97, https://doi.org/10.1016/j.aca.2019.05.016.
[44] M.M. Eteya, G.H. Rounaghi, B. Deiminiat, Fabrication of a new electrochemical sensor based on Au–Pt bimetallic nanoparticles decorated multi-walled carbon nanotubes for determination of diclofenac, Microchem. J. 144 (2019) 254–260, https://doi.org/10.1016/j.microc.2018.09.009.
[45] B.K. Chethana, S. Basavanna, Y. Arthoba Naik, Voltammetric determination of diclofenac sodium using tyrosine-modified carbon paste electrode, Ind. Eng. Chem. Res. 51 (2012) 10287–10295, https://doi.org/10.1021/ie202921e.